Energy Reports 8 (2022) 10072–10087

Contents lists available at ScienceDirect

Energy Reports

journal homepage: www.elsevier.com/locate/egyr

Research paper

Comparative meta-analysis of desalination and atmospheric water harvesting technologies based on the minimum energy of separation

Trevor Hocksun Kwan [a,*], Shuang Yuan [b], Yongting Shen [c], Gang Pei [c]

[a] School of Advanced Energy, Sun Yat-Sen University, Guangzhou, China
[b] Renewable Energy Research Group (RERG), Department of Building Services Engineering, The Hong Kong Polytechnic University, Hong Kong, China
[c] Department of Thermal Science and Energy Engineering, University of Science and Technology of China, China

ARTICLE INFO

Article history:
Received 4 May 2022
Received in revised form 24 July 2022
Accepted 31 July 2022
Available online 13 August 2022

Keywords:
Atmospheric water harvesting
Desalination
Minimum energy of separation
Meta-analysis
Specific exergy consumption

ABSTRACT

Desalination and atmospheric water harvesting technologies are highly desirable to produce freshwater for daily life activities and alleviate the global water crisis. Efforts to improve these have mostly been based on better engineering or materials design, but a comparison of their energy performance over a theoretical optimum is not well consolidated. This research conducts a meta-analysis that comparatively assesses existing atmospheric water harvesting and desalination technologies by evaluating the energy optimality in terms of the Gibbs free energy principle derived theoretical limit. After a review of the various existing technologies in these two classes, energy optimality, defined as the theoretical minimum specific energy consumption divided by the specific exergy consumption, is used as the metric to make a comprehensive and fair comparison of the various desalination and atmospheric water harvesting technologies. Results show that the vapor compression cycle and hybrid technologies-based atmospheric water harvesters have higher energy optimality of 12%, whereas others have much poorer performances of under 3%. For desalination, reverse osmosis yielded the highest energy optimality of 67.43%. Furthermore, the ideal energy optimality needed by atmospheric water harvesting to become comparable to desalination is at least 89.9%, which is almost impossible to practically achieve.

1. Introduction

Water is a crucial resource for human's daily life activities, industries, and agriculture, but it is mostly only utilizable in a highly pure form (e.g. >99.5% w.t.). However, water on Earth exists in many forms as it continuously cycles through the hydrological cycle, where only 2.5% of it is freshwater as it appears due to precipitation (Mendoza-Escamilla et al., 2019). Hence, artificial freshwater separation is a vital industrial practice to increase the freshwater yield as needed by a modern society that has a rapidly growing population. This is a challenging problem because energy consumption, defined by the difference in Gibbs free energy content, is needed to break the molecular bonds between the water and the impurities.

The saline ocean and the atmosphere are the most abundant (but impure) water reserves, thus significant developments have already been made to extract freshwater from them (Yu and Wang, 2022). For oceanic water, extraction methods are generally known as desalination, and its application has dated to as early as the 1600s by British sailors (Belessiotis V., 1999; Woo et al., 2019). Back then, it was achieved by applying heat to force water evaporation into an enclosed chamber, which is later condensed into freshwater by a passive cooling technique. Desalination was first commercialized in 1881 as "Tigne" in Sliema, Malta, and throughout the mid-20th century, modern techniques such as multiple effects distillation (MED) and multi-stage flash (MSF) distillation became the common methods, which exploit a vacuum environment to facilitate water evaporation. Not long after, mechanically driven membrane techniques, often known as reverse osmosis (RO), were also commercialized, such as in 1964 at Lanzarote, Spain. Overall, there is extensive historical development in desalination, so it can be regarded as a relatively mature class of technology.

Meanwhile, freshwater separation from the atmosphere is generally known as atmospheric water harvesting (AWH) (or atmospheric water generation, AWG), which is another trending technique that is useful in regions that lack saltwater reverses as needed by desalination (Hua et al., 2021; Zhou et al., 2020). AWH is principally the same as dehumidification and is different only in terms of the final goal (i.e., retrieving the freshwater).

* Corresponding author.
E-mail addresses: guanxx7@mail.sysu.edu.cn (T.H. Kwan), yuanshuang@mail.ustc.edu.cn (S. Yuan), yongting.shen@connect.polyu.hk (Y. Shen), peigang@ustc.edu.cn (G. Pei).

https://doi.org/10.1016/j.egyr.2022.07.175

Nomenclature

Abbreviations

AWH	Atmospheric water harvesting
ED	electrodialysis
FO	Forward osmosis
GOR	Gain Output Ratio
HD	Humidification–Dehumidification
MED	Multiple effects distillation
MEDAD	Multi-Effect Distillation Adsorption Desalination
MEMD	Multi-Effect Membrane Distillation
MD	Membrane distillation
MSF	Multi-stage flash
PE	Polyethylene
PV	Photovoltaic
RH	Relative Humidity
RO	Reverse osmosis
RR	Recovery rate
SEC	Specific energy consumption
TEC	Thermoelectric cooler
TVC	Thermal vapor compression
VCC	Vapor compression cycle

Variables

C_{salt}	The seawater salt concentration by mass (%)
$\dot{m}_w$	The freshwater flow rate (kg/s)
E_{Min}	Minimum specific exergy consumption (Wh/kg)
E	Specific exergy consumption (Wh/kg)
E_{Heat}	Specific thermal energy consumption (Wh/kg)
E_{elec}	Specific electricity consumption (Wh/kg)
E_{mech}	Specific mechanical energy consumption (Wh/kg)
G_i	The Gibbs free energy of the fluid stream i (J/mol)
$G_{(i,k)}$	The Gibbs free energy of species k of fluid stream i (J/mol)
$h_{(i,k)}$	The specific enthalpy of species k of fluid stream i (J/mol)
$h_{fg}(T)$	The latent heat of specific enthalpy at the boiling temperature T (J/kg)
M_{Salt}	The molar fractions of salt materials
M_{H_2O}	The molar fractions of water
P_o	The ambient pressure (bar)
ϕ_{2nd}	The energy optimality ratio from the 2nd law perspective
Q_{In}	The total heat input (W)
$s_{(i,k)}$	The specific entropy of species k of fluid stream i (J/(mol ·K))
T_0	The ambient temperature (K)
T_H	The input heat's temperature (K)
T_{Sun}	The surface temperature of the Sun (K)
W_{Min}	Minimum work required in a physical separation process (W)

Notably, AWH is a by-product of the common air conditioner because, by cooling the air to below its dewpoint temperature to drop its moisture capacity, freshwater can be condensed and extracted. As a result, the earliest AWH methods, which date to 1947 (Bagheri, 2018a), were based on this air-cooling principle. Such cooling-based AWH technologies have been commercialized in recent years, such as Skywater (Terlouw et al., 2019) and Ecoloblue (Rostamzadeh and Nourani, 2019) as self-sustainable water dispensers. Meanwhile, desiccant-based AWH technology is recently a trending technology in academia (Li et al., 2019), which has commonly been coupled to solar thermal energy (Zhou et al., 2019) by optimizing the interfacial vapor generation energy performance. Yet, even today, a utility-scale AWH platform of any type has never been constructed, and its commercial value has always been much lower than desalination. Specifically, recent exergoeconomic (Alharbi et al., 2020) and techno-economic analyses reveal that the Levelized cost of water is at 6.5 $/m^3 for a state-of-the-art AWH (Siegel and Conser, 2021) but only 0.442 $/m^3 for a regular desalination plant (Moharram et al., 2021b).

Overall, desalination has historically been the most widely applied to obtain freshwater while AWH is still struggling to achieve widespread commercialization. Relevant developments have mostly been focused on optimizing the system's physical structure, material choice, or operating mode to either reduce energy consumption or maximize the water production rate. For example, for desalination, applying multi-objective optimization to determine the plant's optimal geometrical and physical parameters to yield the lowest specific energy consumption (SEC), economic cost, or higher gain output ratio (GOR) is a very common approach (Mahjoob Karambasti et al., 2022), (Beyrami et al., 2019; Tayyeban et al., 2022). These studies often apply a physics model of the specific plant (e.g., (Al-Fulaij, 2011) for multi-stage flash (MSF) desalination) to evaluate the objective terms. Another approach is to assess the desalination plants' techno-economic feasibility, as reviewed by Burn et al. (2015) for agricultural application or by Lin et al. (2021) for those existing in China. Similar to desalination, optimizing the geometrical and physical parameters based on the specific technology's model is also a common approach in AWH research (Zolfagharkhani et al., 2018b; Smejkal et al., 2020), which can be supported by experimental research (Patel et al., 2020; Elashmawy and Alshammari, 2020a). Specific to desiccant-based methods (Ejeian and Wang, 2021), another approach is optimizing the material choice (e.g., ionic liquids (Qi et al., 2019; Wang et al., 2019b), structure, and/or composition. Moreover, a comparison of existing AWH technologies was conducted by Tu and Hwang (2020) using the water harvesting rate (WHR) metric and Chen et al. (2021) for coupling with energy harvesting devices. Nevertheless, despite that desalination and AWH are both freshwater production technologies, a comparison between these two technological classes is very seldom made, and an explanation for their vastly different research trends has yet to be established from a theoretical standpoint. Furthermore, the extent to which the SEC can be optimally minimized in both categories requires clear clarification. In the theory of thermodynamics, the Carnot efficiency is a well-known concept that depicts the theoretical maximum possible energy efficiency for heat-to-power conversion processes. Indeed, a similar analogous theory that depicts the baseline for the minimum energy needed to generate freshwater should exist and be used to assess the optimality of the relevant technologies.

This research uses another perspective to conduct a meta-analysis that compares the feasibilities of AWH and desalination technologies by evaluating their energy optimality in terms of a theoretical limit. Inspired by the theory used by Wang et al. (2020) for only desalination there, the second law-based Gibbs free energy principle is applied to universally evaluate the theoretical energy consumption limit of both AWH and desalination,

which accounts for only the input/output characteristics and ignores any internal influences. Then, the energy optimality term, defined as the minimum SEC divided by the specific exergy consumption, is calculated for each technology, and this enables a comprehensive and fair comparison of the freshwater generation technologies' energy performances. To carry out the analysis, the working principles and research trends of existing AWH and desalination technologies will first be covered in Section 2. The covered technologies shall then be subject to the energy optimality analysis in Section 3. Here, the energy optimality of the common AWH technologies will be compared, and the same comparison is made for the desalination technologies. Afterward, a discussion to cross-compare the performances between AWH and desalination technologies will be made. The methodologies and relevant equations used to evaluate the energy optimality term are detailed in the appendix. Finally, conclusions and recommendations about the more promising technologies will be made in Section 5.

2. Technological review

This section reviews the existing AWH and desalination techniques that will be subject to the energy optimality analysis. Notably, as there are already more detailed technological reviews available in the literature (e.g., please refer to Tu and Hwang (2020) for AWH, and Uddin et al. (2018), Burn et al. (2015) for desalination), the reviews shown here are kept brief and only intended to provide a fundamental understanding of the studied technologies.

2.1. Atmospheric water harvesting

The most commonly known AWH technologies include the condensation-based and desiccant-based methods (Salehi et al., 2020), which are described in detail below. Condensation-based techniques rely on lowering the air temperature to below its dewpoint so that its relative humidity increases to above 100% to force the condensation of water. The required cooling effect can be obtained from any type of cooling device, and the heat pump can be regarded as the most traditional option. Fig. 1 shows such technologies, which include the vapor compression cycle, and the thermoelectric cooler. Notably, Fig. 1 also shows (for both cases) that the uncondensed humid air is fed into the heat pump's hot end, which is a common practice because the heat pump performs better with a lower temperature difference

2.1.1. Cooling based

As the same technology as that used in most buildings' air conditioners, the vapor compression cycle (VCC) is often considered because it has the highest energy performance. For example, studies such as Zolfagharkhani et al. (2018a), Anbarasu and Pavithra (2011) and Patel et al. (2020) have shown its SEC ranges in the 220–300 Wh/kg range while 22–26 L/day can be produced, which can supplement up to 8 occupant's drinking needs. Alternatively, when system simplicity, reliability, and portability are important factors, the thermoelectric cooler (TEC) can be considered because it does not require a compressor or any refrigerants (Lee, 2010). One potential application for a TEC-AWH is being a portable water supply to military personnel during missions in remote regions that lack water reserves but have abundant solar radiation to drive the AWH process (Zhang et al., 2010). Meanwhile, Atta RM (2011) suggested that the TEC-AWH could be employed at land irrigation scales, as they found it could produce 24 L/day in humid areas such as Yanbu. Nevertheless, the TEC has a significantly lower energy performance than the VCC; For example, according to Pontious et al. (2016) who experimentally studied the TEC-AWH, the device had an SEC of 1560 Wh/kg while producing 0.21 L/day. Indeed, these values are much lower than those typically yielded by the VCC-AWH, which is primarily attributed to the lower cooling performance of the TEC.

Notably, besides the heat pump, other types of cooling devices can also be used for the AWH application. One example is the radiative sky cooler (RSC), which is a passive cooling method that uses the outer space environment as the heat sink. Uniquely, Li et al. (2020b) proposed to extend the functionality of solar panels into the nighttime, where the RSC effect is used here to extract atmospheric water by condensation. Besides the PV material, materials that are designed specifically for RSC operation have also been studied, such as two polyethylene (PE) foils (Maestre-Valero et al., 2011). However, several studies also revealed that the freshwater production rate is conversely lower in humid climates, which is because the air RH affects the sky emissivity and consequently reduces the available amount of cooling energy (Khalil et al., 2016; Clus et al., 2008). This dilemma makes the RSC-AWH technology much less practical than the AWHs that use the heat pump. Meanwhile, another cooling option is the absorption chiller (a.k.a. absorption refrigerator) which requires input heat to generate the cooling energy. For better performance carbon footprint-wise, coupling solar-thermal energy is the suitable choice as studied by Salek et al. (2022).

2.1.2. Desiccant based

In the desiccant (also known as sorption) based AWH technology, a certain material with a high capacity for water capture on its body captures water from the atmosphere via a water partial pressure differential. Once this material is saturated, it is regenerated by heating the material (often to 65 °C or above) to evaporate the attached water into an enclosed chamber and later be condensed as the product freshwater. The required heat is commonly supplied by solar energy (Srivastava and Yadav, 2018; Elashmawy, 2020; Elashmawy and Alshammari, 2020b), but it can also come from the waste heat of industrial facilities or fuel cells (Kwan et al., 2020). The aforementioned process is graphically illustrated in Fig. 2. Furthermore, the involved material can be based on absorption or adsorption (Zhou et al., 2020); Absorption involves dissolving or diffusing water into a solution whereas adsorption refers to the sticking of water molecules onto a hydrophilic surface (usually a solid).

Absorption methods generally involve a solution that has a highly hydrophilic salt such as $CaCl_2$ (Talaat et al., 2018; Wang et al., 2019a), LiCl (Gido et al., 2016; Li et al., 2019), where each type of salt has varying water partial pressure profiles with salinity. Alternatively, ionic liquids may also be used, such as [Emim][Ac] as proposed by Qi et al. (2019), which could be regenerated by an interfacial solar-thermal material. To date, these technologies yield water production rates that are generally within the 0.3295 to 0.6310 $L_{water}/(m^2\ day)$ range (Talaat et al., 2018).

For adsorption methods, generally a solid with hydrophilic properties is used, such as silica gel as often used in packaged food to keep them dry. Moreover, other types of adsorbent materials also exist and are being researched, which include the ACF-LiCl compound (Liu et al., 2016), metal–organic frameworks (MOF) (Kim et al., 2017), zeolites, and hydrogels (Lapotin et al., 2020). Generally, these technologies can produce freshwater in the 0.4 to 0.5 $L/(day\ m^2)$ range. Unfortunately, for both absorption and adsorption, such rates are really low when compared to both the cooling-based AWH and the desalination technologies. Indeed, several studies have attempted to improve the performance of these technologies from the structural design and engineering perspectives. For example, Lapotin et al. (2020) demonstrated a dual-stage water harvesting device that would recycle the latent

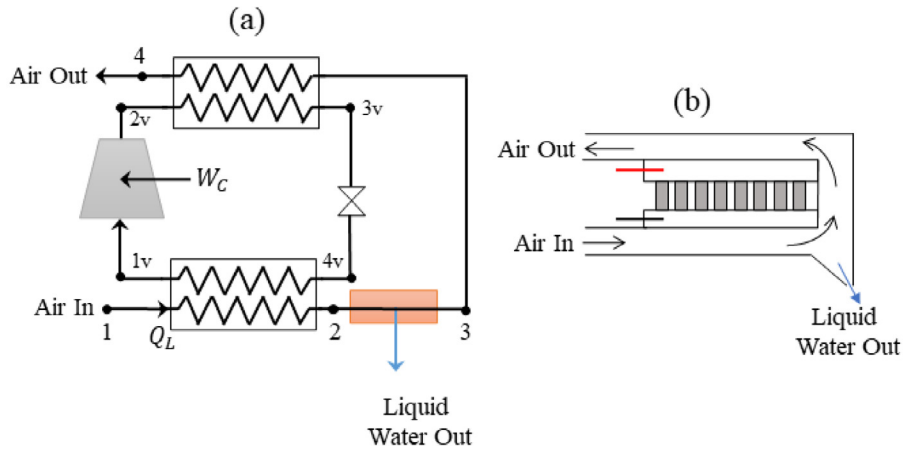

Fig. 1. Schematics of the commonly used condensation-based AWHs involving the (a) Vapor compression cycle (b) Thermoelectric cooler.

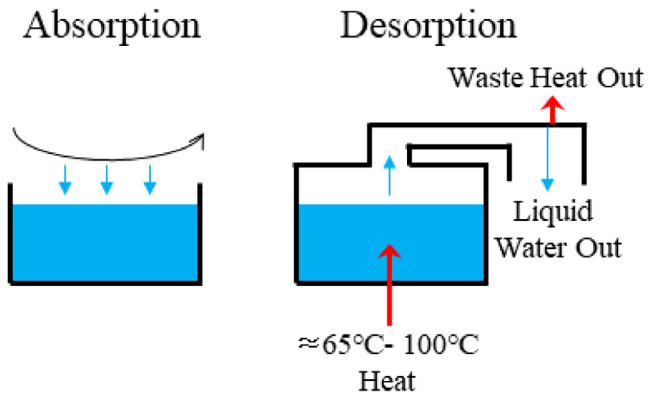

Fig. 2. Schematics of the common desiccant-based AWH.

heat of condensation at the top stage to support the desorption process at the bottom stage. Such a concept enabled freshwater production rates of up to 0.77 L/(m^2 day). Nevertheless, this is still inferior and is inadequate to allow these technologies to compete in the commercial market.

2.1.3. New hybrid technologies

The AWH technologies reviewed up until now involved a single technology, but it is also possible to couple two or more existing technologies to form a hybrid AWH system. To date, hybrid AWH technologies involve a unique configuration, and several examples have been identified as follows. Fill et al. (2020) applied conventional liquid desiccants (e.g. $CaCl_2$) to capture water from the atmospheric air. However, instead of conventionally applying heat, the liquid desiccant is instead regenerated via reverse osmosis, which is a common desalination technique. Tu and Hwang (2019) coupled the VCC (or heat pump) to the desiccant wheel, where the desiccant wheel is located upstream to pre-humidify dry (RH < 15%) air before cooling to condense water at the heat pump's evaporator. Al Keyyam et al. (2021) proposed an absorption chiller-based AWH device, where the power and heat sources are the concentrated photovoltaic – thermal (CPV/T) and Stirling engine devices.

2.2. Desalination

Currently, the most commonly known desalination technologies include thermal-based, membrane separation-based, and humidification–dehumidification-basedmethods. These technologies will be reviewed in the following subsections.

2.2.1. Thermal based

Thermal-based desalination separates water from salt by exploiting the liquid–vapor phase properties of the water. Similar to natural rain, thermal-based desalination applies thermal energy to cause water evaporation, and water vapor is later condensed at a separate location for collection. The thermal energy may originate directly from electric heating, or it can be cleanly produced by solar thermal collectors (Cunha and Pontes, 2022) or from the waste heat of gas turbine cycles. The commonly known thermal-based desalination technologies include Multi-effect distillation (MED) and Multi-stage flash (MSF) (Kavitha et al., 2019) whose typical structures have been illustrated in Fig. 3. In both cases, the enclosed chambers are often subject to a vacuum environment because this reduces the water boiling temperature and increases the water evaporation rate. The vacuum environment is typically created by installing a vacuum pump for each stage of the plant, which runs to remove any non-condensable gases.

Fig. 3 (a) shows a typical structure of the MED with 3 stages, noting that the number of stages can be arbitrarily chosen in design. In each stage, water is separated by transferring heat from superheated steam into the seawater, and the superheated steam originates from the last stage (3 in Fig. 3(a)) of the MED plant. This steam can be heated either by mechanical or thermo-compression methods. As the steam transfers heat with the seawater, it condenses into the freshwater product for collection. MED is historically the first commercialized desalination technology, which is especially true for the Chinese desalination market (Lin et al., 2021). In recent years, numerous efforts have been made to optimize the performance of the MED plant (Abid et al., 2021a), such as coupling it with a thermal vapor compression system (Elsayed et al., 2018a), utilizing the waste heat of wind turbines (Khalilzadeh and Hossein Nezhad, 2018), or solar thermal technologies (Ghenai et al., 2021).

Fig. 3 (b) shows the typical structure of the MSF plant, which, similar to the MED plant, can involve any number of stages (3 is shown in the diagram). In this design, the seawater is pre-heated by exchanging heat with the superheated steam long at each stage of the plant serially. Afterward, the seawater is then heated in a boiler to the temperature required for a rapid rate of water evaporation, which is then passed serially in the opposite direction to the incoming seawater. Compared to MED, MSF has been more successful because it has a simpler layout and a more reliable performance (Sharaf Eldean and Fath, 2013). Previous studies have shown that the MSF performance can be optimized by increasing the top brine temperature, the number of stages, and the specific heat transfer area ((Sharaf Eldean and Fath, 2013), (Rosso et al., 1996)). Furthermore, similar to the MED plants, the

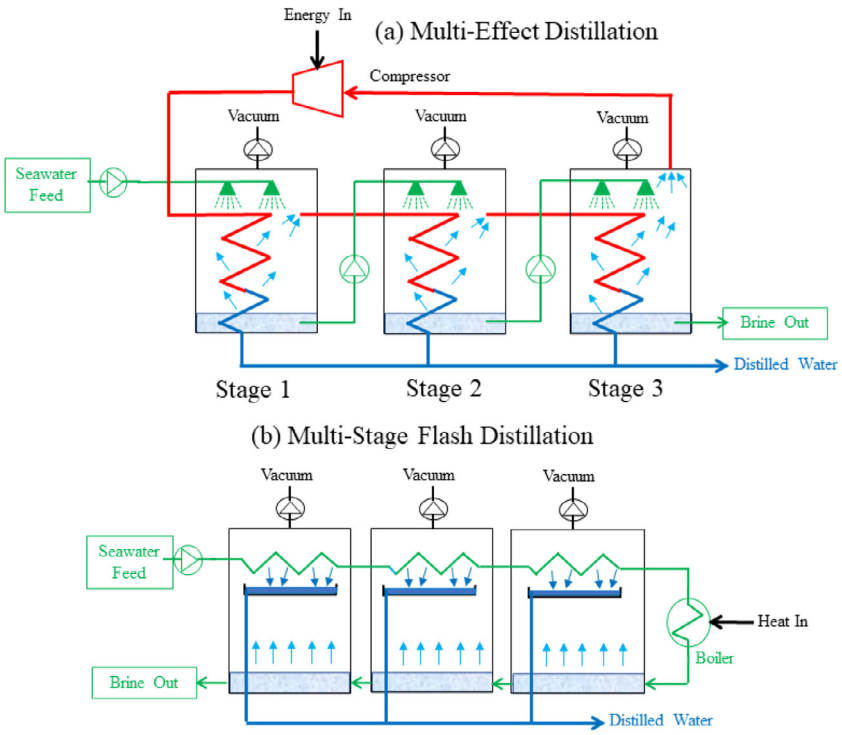

Fig. 3. Schematics of the common thermal-based desalination technologies.

coupling of solar thermal energy to MSF plants is also a common practice (Moharram et al., 2021a).

Indeed, other innovative thermal-based seawater to thermal desalination also exist, such as the forward osmosis pretreatment method (Altaee et al., 2014) that removes divalent ions from seawater by an osmotic pressure gradient. Another relatively recent concept is the multi-effect membrane distillation (MEMD), which combines the reverse osmosis and the multi-effect distillation (MED) principles (Boutikos et al., 2017; Hassan et al., 2020); The seawater is heated until its water partial pressure difference is significantly above the permeate side of the membrane. Doing so generates water vapor that crosses the hydrophobic membrane to the permeate side, which is later condensed and retrieved as the product freshwater. Notably, the liquid components cannot pass the hydrophobic membrane because of the high surface tension of the polymeric membrane materials (El-Zanati and El-Khatib, 2007). MEMD has been proven to have higher thermal efficiencies than the single-stage membrane distillation system (Pangarkar and Deshmukh, 2015; Zhao et al., 2013).

Overall, thermal-based desalination has the advantages of relatively low pretreatment requirements, high system reliability, and flexibility (Jamil and Zubair, 2018; Shahzad et al., 2018). However, these methods are also energy and cost-intensive and have relatively high carbon footprints (Ghaffour et al., 2013), so although they are commercially competitive, they are not a predominant freshwater extraction technique.

2.2.2. Membrane based

The technologies of membrane separation-based desalination include reverse osmosis (RO) and electrodialysis (ED) methods (Al-Karaghouli and Kazmerski, 2013). Amongst these, reverse osmosis is a mature product that has already been commercialized for many decades. Its basic structure is shown in Fig. 4 which involves a membrane that passes water but blocks the salt molecules. The water can pass through the membrane when the solution is pressurized to above its osmotic pressure (varies with the salinity concentration) and is later collected as the desired product [39]. In comparison to the thermal desalination methods, reverse osmosis generally has a lower energy consumption with SECs as low as 2.1 Wh/kg (El Mansouri et al., 2020), and it is a mature technology whose installed capacity ranges between 100 L/day (used in marine and household applications) to 395,000,000 L/day (as a regional artificial water source) (Al-Karaghouli and Kazmerski, 2013). Notably, coupling reverse osmosis with solar power is a common approach to eliminating the otherwise carbon footprint caused by fossil fuel combustion (Geng et al., 2021; Shalaby et al., 2022). However, the adopted membrane material is often not perfect and may leak a small amount of the salt ions into the permeate freshwater. As a result, RO-based desalination is less ideal when extremely highly pure water is required or if the seawater concentration is higher than the average oceanic values (roughly 3.5%). Thus, many Middle Eastern countries still tended to prefer thermal desalination because the seawater quality from the nearby Red Sea is very low (Hanshik et al., 2016).

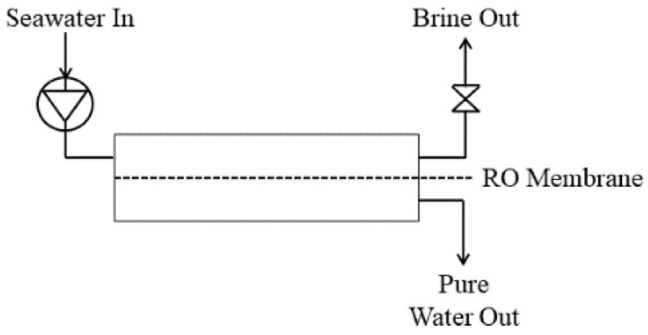

Fig. 4. Schematic of the reverse osmosis-based desalination technology.

2.2.3. humidification–dehumidification based

The HD desalination system's working principle is shown in Fig. 5, which works by emulating the natural hydrological cycle and the "precipitation" stage is the location of freshwater

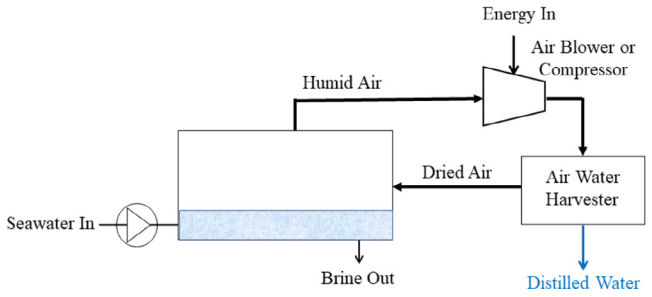

Fig. 5. Schematic of the HD-based desalination technology.

collection (Ashrafizadeh and Amidpour, 2012). Initially, dry air and seawater are fed into the "humidification" chamber, where water evaporation from the seawater humidifies the air to an RH of ideally 100%. Then, through a blower or an air compressor, the humid air is passed over to an air–water harvester device to collect the product freshwater. Notably, the air–water harvester is technologically identical to any type of AWH, so the overall efficiency of this method is constrained by the AWH's performance. Meanwhile, the water productivity of this method can be enhanced by preheating the dried air or seawater to enhance the water evaporation ability at the first stage (Santosh et al., 2022), which may be provided by either solar thermal collectors or industrial waste heat (He et al., 2016). Another suggested methodology is applying a heat pump, where the generated cooling energy can be further used to facilitate the dehumidification process (Lawal et al., 2018a).

3. Generic minimum SEC model

Fig. 6 shows the structure of the minimum specific energy consumption (SEC) model that is universally used to evaluate the minimum SEC of all freshwater extraction technologies, which has been used previously by textbook (Seader et al., 1998), (Wang et al., 2020) for desalination and (Zhao et al., 2017) for carbon capture. Here, the feed stream (1) is given as an input to the physical separation process, while the output is the captured stream (2) that contains the desired product, and a waste stream (3) that contains the uncaptured constituents of the feed stream. All fluid streams contain a thermodynamic potential, known as the Gibbs free energy, which defines the theoretical amount of reversible work that is contained within the stream. Generally speaking, liquids or gases will always naturally flow towards the state of lower Gibbs free energy as they prefer to be in a mixed state. Therefore, a certain amount of work (W_{Min}) is required in any physical separation process to counter the state of mixing caused by natural diffusion, which is defined as the difference in the Gibbs free energy state between the feed stream and the two output streams. Mathematically, W_{Min} is defined as follows:

$$W_{Min} = n_2 \cdot G_2 + n_3 \cdot G_3 - n_1 \cdot G_1 \tag{1}$$

where n_i and G_i are the molar flow rates (mol/s) and the Gibbs free energy (J/mol) of the fluid streams, respectively, with i to identify the fluid stream of interest. The parameters n_i and G_i are vectors that contain the molar flow rate and Gibbs free energy of each species contained within the fluid stream (i.e., $n_i = [n_{(i,1)}, n_{(i,2)}..n_{(i,k)}]$ and $G_i = [G_{(i,1)}, G_{(i,2)}..G_{(i,k)}]$). In a generalized reversible physical separation process that does not involve any chemical reactions, the Gibbs free energy can be defined as:

$$G_{(i,k)} = h_{(i,k)}\left(p_{(i,k)}, T_0\right) - T_0 s_{(i,k)}\left(p_{(i,k)}, T_0\right) \tag{2}$$

where $p_{(i,k)}$ is the partial pressure of species k of fluid stream i, which is directly proportional to the fluid stream's total pressure and the molar fraction of species k (i.e. $p_{(i,k)} = y_{(i,k)}P_0$). Notably, if the species involved in all of the fluid streams are ideal gases, then the Gibb's free energy expression can be simplified to the equation previously reported by Zhao et al. (2017). However, this simplified expression no longer holds if non-ideal gases or liquids are involved (as of this paper's case studies). Instead, the specific enthalpy and entropy expressions of Eqs. (2) shall be calculated by using the thermophysical properties of the species of existing lookup tables, which are available in commercial software packages such as NIST or CoolProp (The latter is used in this paper).

Based on the minimal power consumption W_{Min}, the theoretical minimal SEC of the separation process can also be derived as follows:

$$E_{Min} = \frac{W_{Min}}{n_{(2,k_{H_2O})}} \tag{3}$$

where parameter $n_{(2,k_{H_2O})}$ is the molar rate of pure freshwater as the desired product. This parameter has default units of W/mol (which can be easily converted into Wh/kg, etc.). Effectively, E_{Min} serves analogously like the Carnot efficiency limitation for freshwater separation.

The energy optimality ratio is defined as follows:

$$\phi_{2nd} = \frac{E_{Min}}{E} \tag{4}$$

where E is the equivalent specific exergy consumption of the freshwater separation technology, which should be evaluated by knowledge of the reported SEC data by the reference. Conversions from SEC to E should be made by applying the appropriate equations presented in Appendix A3 depending on whether the input was heat, electricity, or solar energy. Parameter ϕ effectively quantifies the optimality of the freshwater separation device; A value of 1 indicates the system has a perfect performance while values approaching zero (e.g. < 1%) indicate a poor energy performance.

For freshwater separation, the captured stream is considered to be pure water (i.e., molar flow rates of the other constituents equal zero) whose amount is defined as a certain percentage (described as the recovery rate, RR) of that existing in the input stream, as shown below:

$$n_{(2,k_{H_2O})} = RR \times n_{(1,k_{H_2O})} \tag{5}$$

From this, the molar rates in the waste stream are known by conservation of mass to be: $n_3 = n_1 - n_2$. Indeed, the application of the above generic SEC model requires that the commonly used metrics to describe water content in the AWH and desalination applications be translated into molar rates. The methods to achieve these are described in the following subsections.

4. Energy optimality analysis

The cases for AWH and desalination will first be separately analyzed. Here, the energy optimality ($\phi_{2nd} = \frac{E_{min}}{E}$) term will be used to compare the theoretical performance of the various well-known freshwater separation technologies. The term E is the "specific exergy consumption" of the technology and is calculated based on the energy data as reported by the authors, which may be electricity, solar energy, heat at a given temperature, etc. The conversion equations to obtain exergy from energy are listed in Appendix A4. The SEC requirement curves are generated under the varying water content (RH and salinity concentration, C_{Salt}, respectively), temperature, and other conditions. The covered AWH

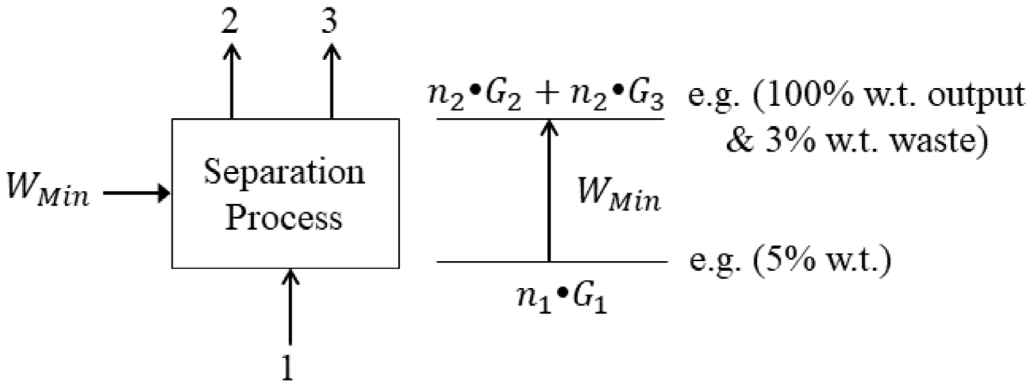

Fig. 6. Schematic of the generalized physical separation process. In the left diagram, 1 is the feed stream, 2 is the captured stream, and 3 is the waste stream. In all fluid streams, the mixture may be a liquid or a gas.

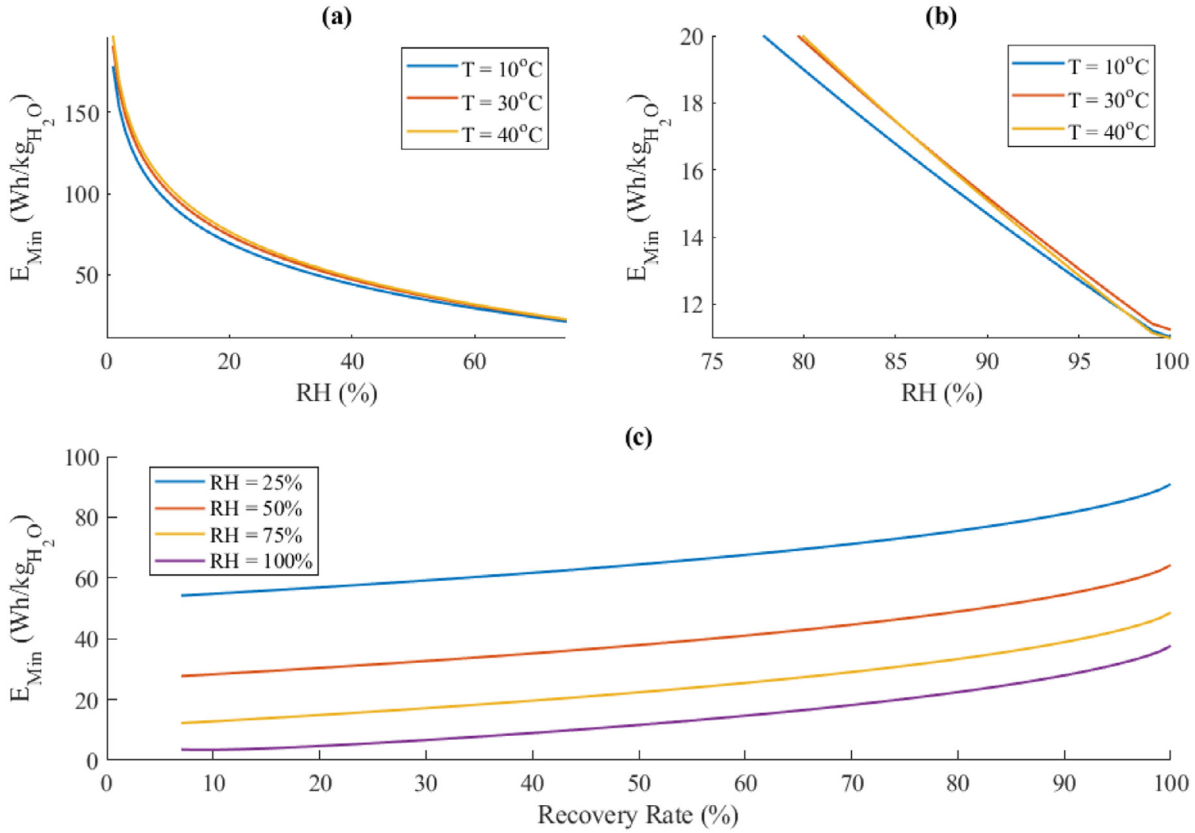

Fig. 7. Curves showing how W_{min} changes in the AWH scenario with the ambient RH ranging from 0% to 75% and 75% and 100% in (a) and (b), respectively, which are shown separately for better visuality. In graphs (a) and (b), the recovery rate is fixed at 50%. In graph (c), the recovery rate is varied while the temperature is fixed at 25 °C. In all graphs, the ambient pressure (P_0) is 1 bar.

technologies include the vapor compression cycle (VCC), the thermoelectric cooler (TEC), solar-thermal assisted desiccants (both liquid and solid based), and recent hybrid technologies (HT). For desalination, there will be multi-effect desalination (MED), multi-stage flash (MSF), multi-effect membrane distillation (MEMD), reverse osmosis (RO), and humidification–dehumidification (HD) methods. Notably, in the desalination application, the gain output ratio (GOR) may often be used to quantify energy performance. In this case, the formulas presented in the appendix (A1 and A2) can be used to convert GOR into SEC. Finally, a comprehensive comparison between AWH and desalination based on ϕ_{2nd} is conducted.

4.1. Case atmospheric water harvesting

4.1.1. Minimum SEC requirement

The effects of the relative humidity and different typical ambient temperatures on the E_{min} requirement are explored. Later, the effect of the atmospheric pressure is also studied to simulate the case of capturing water at higher altitudes. Afterward, comparisons of the E_{min} values with practical SEC values of real AWH devices are made. Fig. 7 shows how the E_{Min} value varies with different RH, ambient temperature, and recovery rate values when separating from atmospheric air. Clearly, E_{Min} experiences an almost exponential like increase as the RH approaches 0%,

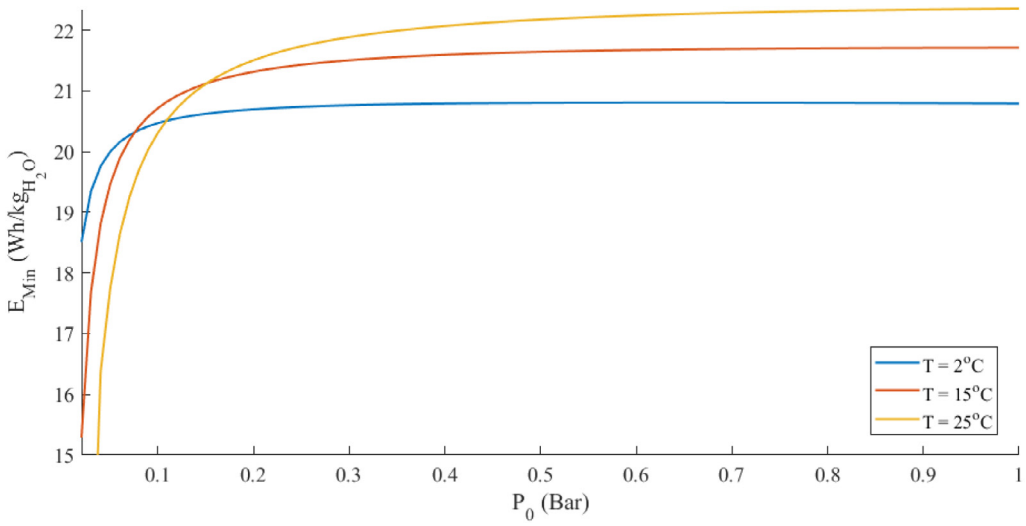

Fig. 8. Curves showing how W_{min} changes in the AWH scenario with atmospheric pressure (P_0) while the RH is fixed at 75% and the recovery rate is 50%.

where up to 150 Wh/kg is needed when RH is 5%. This is expected as a lower RH involves a much lower water vapor concentration, and E_{min} would obviously be infinity if water is not present. On the other hand, a higher RH requires a remarkably low E_{Min}, where values are around 8 to 20 Wh/kg for RH > 75%, which is potentially 4 times lower than when the RH is under 40%. Meanwhile, a higher ambient temperature will generally increase E_{Min} but with not higher than 5% difference. These trends support the commonly known concept that AWHs are best used in very humid environments.

Fig. 8 shows how E_{Min} changes with atmospheric pressure (P_o) and three temperature choices, which indirectly depict how the AWH's minimum energy requirement changes with altitude. Generally, E_{Min} will generally decrease as P_o decreases, but very little influence is observed when P_o is above 0.2 bar. This occurred likely because at these levels, P_o has a weak influence on the specific enthalpy and entropy of the gas and water constituents, thus producing tiny differences to the involved Gibbs free energy terms. In contrast, a rapid drop in E_{Min} is found as P_o drops below 0.1 bar, which is likely the result of the drop in the specific enthalpy and entropies of the constituents as they begin to approach the vacuum condition.

Overall, both a lower P_o and lower ambient temperature are characteristics consistent with those of atmospheric air at increasing altitudes, and both trends lower E_{Min}. Subsequently, applying AWH inside the "atmospheric rivers" which are typically at several kilometers' altitudes above ground or at mountain tops where the "atmospheric rivers" are located, a concept that is commonly known as "artificial rain" (Chernikov), is a potential practical choice from the energy consumption perspective.

4.1.2. Energy optimality estimation

Fig. 9 shows how ϕ_{2nd} and the equivalent E (based on reported conditions) compare between the various AWH technologies and individually amongst different references. According to these results, the thermoelectric cooler based AWH typically has a very low ϕ_{2nd} values that is at most 3.03% by reference 3 with a corresponding equivalent E of 769 Wh/kg. The most efficient case is most likely representative of an optimized system and a TEC with relatively good quality thermoelectric properties was applied. The other studies have reported SECs that are generally in the 1500–2500 Wh/kg range, but the SEC is not very sensitive to the operating temperature and RH condition. However, as E_{Min} is lower with a higher RH condition, this causes a lower ϕ_{2nd} result amongst the reported TEC-AWH solutions. In other words, the TEC-AWH does not necessarily perform better in the RH = 80% environment over RH = 60%, which is likely because its cooling capacity is limited.

Meanwhile, these results show that the VCC has a rather large deviation in the ϕ_{2nd} and equivalent E values ranging from 1.8%–12% and 300–840 Wh/kg, respectively. The large swing of ϕ_{2nd} is likely due to the differences in their technological design factors, such as the choice of refrigerant, the condenser, and evaporator heat exchange designs, and so on. Nevertheless, the reported ϕ_{2nd} value of 12% represents the second-highest amongst all of the other AWH solutions (with reference 18 occupying the highest), which indicates the VCC-AWH is currently the best performing solution. This is likely because the VCC has a high coefficient of performance for producing cooling energy. Nevertheless, a maximum of only 12% indicates that the VCC-AWH technology still has room for optimization. There are two suggestions for which this can be achieved; Firstly, the waste heat at the condenser end of the VCC could be used for further AWH operation, such as regenerating a desiccant-based AWH technology. Secondly, further efforts to optimize the condenser heat exchanger design to better extract the freshwater can be made.

The ϕ_{2nd} values for solar-assisted desiccant AWHs are roughly in the 1.26%–1.82% range with equivalent E values ranging from 1200 Wh/kg to 3000 Wh/g. There is also an extreme outlier of reference 13 (Elashmawy, 2020) with a ϕ_{2nd} value of only 0.18%, which indicates the experimental platform designed used in Elashmawy (2020) was not well optimized. Overall, the better-performing cases have a slightly higher performance than the TEC-AWHs, but even these cases are very inferior to the VCC and suggest the solar-driven desiccant-AWHs are not an ideal solution. The low efficiency is due to the conversion of solar energy into low-temperature heat before it is later converted into energy for collecting freshwater. This is very problematic because low-temperature heat has very low exergy content; For instance, if heat at 350 K (76.85 °C) is applied to extract freshwater in 300 K (26.85 °C) humid air, then based on the Carnot efficiency formula, only 14.29% of the solar energy can theoretically be converted into work for freshwater separation. Note that this value assumes that the entire process is 100% thermally efficient, which factors that the heat-to-work conversion process is perfect and that thermal losses do not exist. Indeed, this is generally almost impossible to achieve realistically. Furthermore, even for the 100% thermal efficiency scenario, the resulting 14.29% efficiency is only slightly

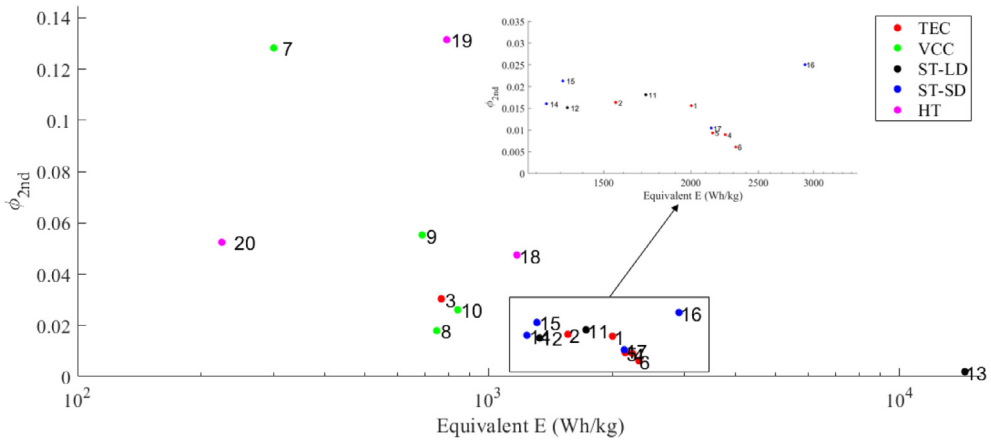

Fig. 9. Comparison of the ϕ_{2nd} and the equivalent exergy consumption (based on reference data) between the various AWH technologies. The different colors identify the technology type being plotted, and the numbers shown beside the dots are the ID numbers to identify the reference the reported E originated from, as listed in Table A.2 (Appendix A4).

higher than the VCC-AWH, and it is also lower than the average electrical efficiency of state-of-the-art PV technologies. Considering that current VCC-AWH technology still has plenty of room for further optimization, it is unlikely that a fully optimized solar-driven desiccant-AWH can eventually reach competitive energy efficiencies. Furthermore, the absorption stage of the desiccant based AWH method conversely increases the absorbed water's Gibbs free energy gap relative to the pure water, which increases the theoretical E_{Min} (this factor will be clearer when analyzing the influence of C_{salt} in Fig. 10). Hence, a major contradiction exists in that adopting desiccants of higher concentrations to extract from drier air will conversely further increase E_{Min}. This problem worsens when desiccant based AWHs are used in arid environments with RH being typically around 30% (Hua et al., 2021), a scenario in which E_{Min} is already a relatively large value. All in all, the solar-driven desiccants are not recommended as a sustainable AWH technology because of the above two thermodynamic limitations.

On the other hand, the HT based AWHs have considerably different ϕ_{2nd} and equivalent E performances, but they overall demonstrated comparable ϕ_{2nd} values with the VCC-AWH. Observing reference 14 (Fill et al., 2020) of Fig. 9 that coupled water absorption to reverse osmosis, the ϕ_{2nd} is found to be significantly higher than the TEC and desiccant AWHs but still inferior to the VCC-AWH. Most likely, like the desiccant solution method, the primary factor that constrains this method's 2nd law energy optimality is the lower Gibbs free energy value of water in highly concentrated salt over that in the humid air. Notably, reference 18, which coupled the VCC to the desiccant wheel, remarkably yielded the highest ϕ_{2nd} performance amongst all studied references of 13.16%. This high performance can be attributed to combining the better performing VCC and applying its waste heat to regenerating the desiccant wheel. Finally, reference 19, which involved a CPV/T-Stirling engine powered absorption chiller, though yielding the lowest equivalent E of 225 Wh/kg, had a lower ϕ_{2nd} because it was working under a much more ideal condition of RH = 100% at 40 °C. Besides, the lower ϕ_{2nd} for this case is also likely attributed to the high complexity of their proposed system which made it difficult for one to evaluate the ideal working conditions. Overall, the analysis has demonstrated that HT based AWHs can potentially yield better ϕ_{2nd} values than even the best VCC-AWH technology, so this is potentially a good direction for further development.

4.2. Case desalination

4.2.1. SEC requirement

Fig. 10 shows how the E_{Min} value varies with different salinity concentration (C_{Salt}), ambient temperature, and recovery rate values when separating from saline water. Unsurprisingly, the E_{Min} value starts from zero at $C_{Salt} = 0$ and rapidly increases with C_{Salt}. More precisely, at lower salinity levels (such as 3.5% for natural oceanic water), the E_{Min} value is a relatively small value of around only 1.5 Wh/kg. These values are much smaller than those encountered in Fig. 7 for separating water from humid air, thus explaining why freshwater separation from seawater requires much lower energy consumption. The reason for a lower E_{Min} is most likely because the water concentration at such low C_{Salt} values is very high over that in humid air. According to Fig. 10(c), E_{Min} is relatively steady with the recovery rate up until 60%, but a sudden increase is observed as the recovery rate approaches 100%; For example, the E_{Min} value rapidly increased from 3.5 Wh/kg to 25 Wh/kg for the $CaCl_2$ curve from 60% to 100% recovery rate. Most interestingly, between the two salts, $CaCl_2$ requires a lower E_{Min} for all working conditions. Here, the E_{Min} value between the two salts is decided by two factors; $CaCl_2$ has a higher specific enthalpy and entropy than NaCl, which increases its Gibbs free energy value, but $CaCl_2$ has a much higher molar weight (almost double of NaCl), which lowers its relative molar fraction with C_{Salt} in the solution. Clearly, the latter factor had the larger influence to lower $CaCl_2$ solution's E_{Min} value to below that of NaCl.

4.2.2. Energy optimality estimation

Fig. 11 shows a comprehensive comparison of the reported equivalent E and ϕ_{2nd} values between the various desalination technologies. For the MED, MSF, and MEMD technologies, the values generally increase with increasing the number of effects in their technologies. This is consistent with the reported trends by previous studies for thermal-based desalination technologies (e.g. Ma et al. (2020)) because more effects increase the utilization rate of the applied heat; The "waste heat" from each stage is progressively passed and recycled to the next stage. Furthermore, between the MED, MSF, and MEMD, for the same number of effects, the ϕ_{2nd} magnitudes are similar and no obvious differences is observable. For example, between references 8 (Rosso et al., 1996) and 10 (Ma et al., 2020) that adopted 16 and 14-effect

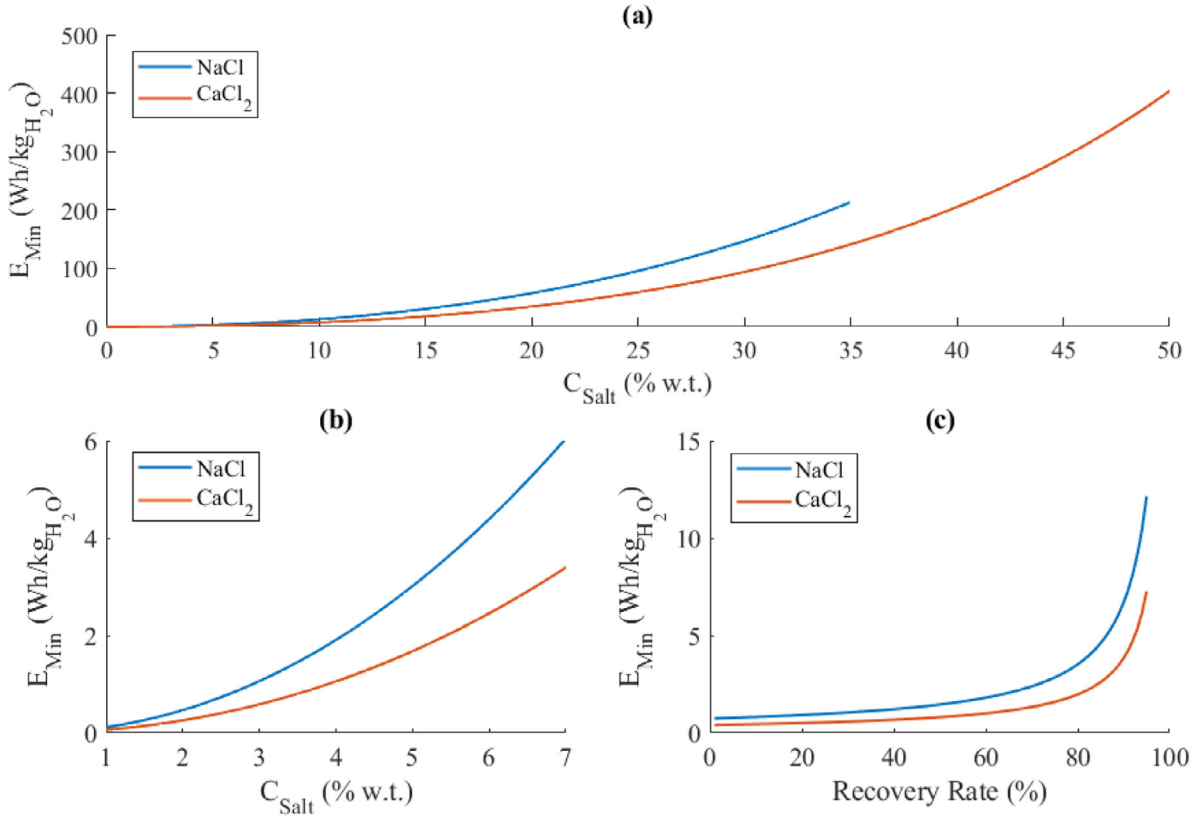

Fig. 10. Curves showing how E_{min} varies when freshwater is separated from salt solutions with (a) C_{Salt} while the recovery rate is fixed at 50% (b) The same as (a) but presenting C_{Salt} in the range of 1%–7%, which is more representative of seawater concentration levels and (c) Varying recovery rates while C_{Salt} is fixed at 3.5%. In the presented cases, the temperature is fixed at 25 °C.

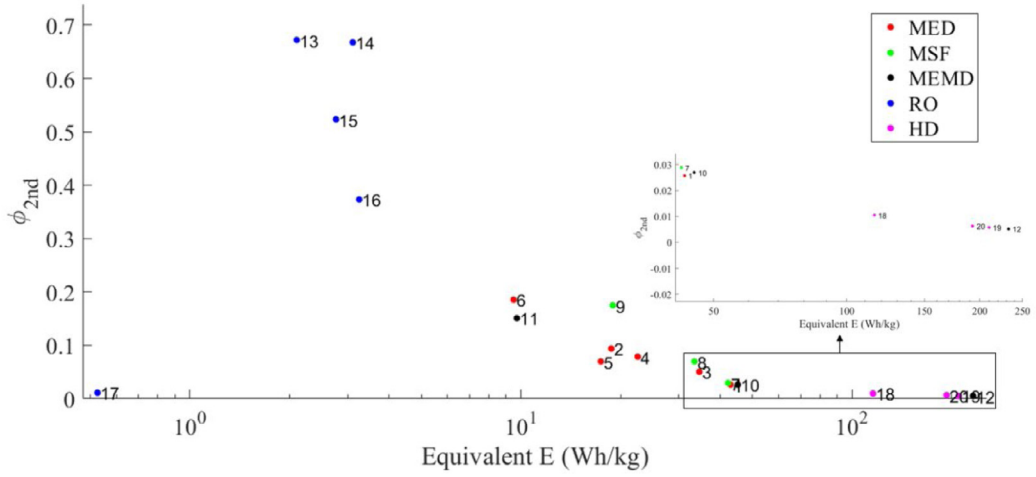

Fig. 11. Comparison of the ϕ_{2nd} and the equivalent exergy consumption (based on reference data) between the various desalination technologies. The different colors identify the technology type being plotted, and the numbers shown beside the dots are the ID numbers to identify the reference the equivalent E originated from, as listed in Table A.3 (Appendix A4).

plants, the values are generally close to 10%. Uniquely, reference 5 (Ghenai et al., 2021) presented a comparison of the energy consumption between conventional solar-driven MED plants, and their newly proposed solar-driven MED and adsorption hybrid plant. The analysis here has verified their study's observation that hybridizing the adsorption method has greatly increased their

plant's ϕ_{2nd} from 9.37% to 18%, which is mostly likely due to the improved solar energy utilization efficiency by their hybrid system.

For reverse osmosis, Fig. 11 shows that, except for Cerci (2002), the RO technique has shown a very high ϕ_{2nd} performance. This is inherent because the driving force for freshwater separation is directly by mechanical energy, so the irreversible losses involved in most typical heat to work processes are eliminated, and mechanical energy loss is easier to suppress than heat loss. Remarkably, two references registered ϕ_{2nd} in the 37%–40% range while another two are above 50%, and the maximum is 67.43% for reference 12 (El Mansouri et al., 2020). The differences are likely because the better cases used a better-quality membrane that had lower pressure head losses for passing water. Remarkably, the low performance was observed for reference 16 (Cerci, 2002) of only 1.16%. This is likely because the end application of their work is the desalination of brackish water (hence why the chosen C_{Salt} condition is 0.155%), which involves more complicated ion constituents than NaCl and $CaCl_2$ as studied in this paper, and brackish water also contains suspended particles that could affect the RO performance.

Meanwhile, the HD method generally has the lowest ϕ_{2nd} (values below 1.3%) amongst all of the desalination technologies. This is because this method uses humid air as the transfer medium for freshwater, so the air–water harvester is technologically identical to the AWH. This means the overall efficiency of this method is constrained by the AWH's performance and can never be better than it. Indeed, this system could be further optimized by maximizing the energy utilization efficiency of the input heat or adopting a more efficient dehumidification technology such as those based on the Electro-osmosis concept. Nevertheless, it is already established previously that the E_{Min} of AWH technologies is typically higher than desalination, the possibility that the HD technology can be optimized to commercial-grade quality is predominantly low. Thus, further research on the HD method may not necessarily have significant research value.

Overall, the RO method yields the highest ϕ_{2nd} amongst all studied technologies with values averaging in the 39% range and peaking at 67%. Even with the highest number of effects by MED, MSF, and MEMD methods, their ϕ_{2nd} values could not exceed 30%. Thus, the RO method appears to be the most attractive freshwater technology. Increasing the practicality of the RO method, such as minimizing its salt leakage, increasing the membrane lifetimes, etc., is recommended.

4.3. Comparison between AWH and desalination

By comparing the results in Figs. 7 and 10, one will find that AWH generally has a much higher E_{min} than desalination. Specifically, by comparing the reported values, the E_{Min} values for the AWH technology generally range from 17 Wh/kg for favorable conditions (e.g., high RH) to up well beyond 100 Wh/kg in harsher (e.g., low RH) conditions. In contrast, for desalination involving oceanic salinities, the E_{Min} values are generally all lower than 4 Wh/kg, which is over 3 times lower than even the most favorable working conditions for extracting freshwater from the air. Notably, the lower E_{Min} values for oceanic waters also supports the natural preference for water evaporation into the atmospheric air as a higher E_{Min} is indicative of a lower equivalent water concentration. On the other hand, solar heating is still needed to cause precipitation as it accelerates the water evaporation rate beyond the available moisture capacity, hence causing an effect similar to that seen in humidification–dehumidification desalination.

Besides E_{Min}, the ϕ_{2nd} values for the more mature desalination technologies are also generally higher (e.g., around 25% for thermal-based and over 39% for membrane-based). This is an interesting observation, especially for thermal-based desalination technologies since most AWH technologies are also thermally driven. This may be because existing desalination techniques have already undergone significant optimization, such as utilizing a vacuum environment and employing multiple thermal stages to maximize the utilization of the heat. Furthermore, mechanical based techniques such as RO have even higher and dominant ϕ_{2nd} values than all AWH technologies, which is predominantly because RO methods avoid the usage of heat. Overall, both the lower E_{Min} and higher ϕ_{2nd} trends of desalination make this a much less energy-consuming process than AWH, which explains why desalination has always been the more successful technology.

Moreover, in the desiccant-based AWH technology, a highly concentrated salt solution involving highly hydrophilic salt such as $CaCl_2$ is often used to capture water, and the solution is later regenerated to retrieve the freshwater. However, according to Fig. 10, the SEC for freshwater separation from a $CaCl_2$ exceeds 100 Wh/kg when C_{Salt} is over 30%. As verified in Fig. 7, this is the equivalent SEC value of an AWH technology working with an RH of around 15%. The SEC would also further rise to as high as 420 Wh/kg at the crystallization limit of around 50%, which would equate to humid air with an RH value even lower than 1%. In other words, adopting a highly concentrated hydrophilic salt solution to achieve AWH conversely increases the process's SEC. These trends likely explain the extremely low freshwater production rate of current desiccant-based AWHs (Wang et al., 2019a; Qi et al., 2019), so this is not a sustainable technological route for long-term development.

Furthermore, a brief calculation will show that, even after a thorough technological optimization, the AWH technology is still unlikely to become competitive with state-of-the-art desalination technologies in terms of minimal energy consumption. Specifically, consider the typical MSF desalination technology ((Rosso et al., 1996) (16-effect) case, which had the values $E_{Min} = 3.942$ Wh/kg and $E = 15$ Wh/kg, which equates to $\phi_{2nd} = 26.28\%$. Then, let us consider the AWH technology studied by Patel et al. (2020) whose working condition was $T = 35\ ^{\circ}C$ and RH $=$ 95%, which gives $E_{min} = 13.49$ Wh/kg. From this, the theoretical ϕ_{2nd} value required to make the AWH technology have the same $E = 15$ Wh/kg value as the aforementioned MSF technology is calculated to be 89.9%. This is an extremely challenging value to reach, where, as shown in Fig. 9 even the best AWH technology yields a performance of 12% (by Zolfagharkhani et al. (2018a) that is nowhere near this. As a result, desalination should always be preferred over AWH when there is a water reserve available.

5. Conclusion

In summary, a comparative energy performance analysis of various existing freshwater separation technologies (both desalination and atmospheric water harvesting (AWH)) has been conducted. After a brief technological review of both classes, the energy optimality ratio ($\phi_{2nd} = E_{min}/E$) term is defined for the comparative analysis, where E_{Min} is the theoretical minimum energy consumption as derived from the Gibbs free energy principle, and E is the equivalent specific exergy consumption that is calculated based on energy consumption data provided by the studied references. The conducted analysis has shown that:

1. Amongst the various AWH technologies, the vapor compression cycle (VCC) yields the highest ϕ_{2nd} values, peaking at 12% because the VCC exhibits a higher coefficient of performance (COP) values. On the other hand, AWH systems based on hybridizing multiple technologies have demonstrated comparable performances, so this is a suitable direction for further development.

2. On the other hand, thermoelectric cooling (TEC) and desiccant based AWHs have much poorer ϕ_{2nd} performances with

the highest being 3.03% to date. This occurred because of the low COP of TECs, and desiccants needed to be in highly concentrated solutions that significantly increase the E_{Min} requirement over what is already a large value for AWH.

3. For desalination, thermal-based methods (e.g., multi-effect, multi-stage, etc.) have moderate ϕ_{2nd} values that are typically 10% to 20%. Meanwhile, reverse osmosis (RO) has the highest ϕ_{2nd} of 67.43% because it did not need to convert heat into work, so this is the most suitable technology for further optimization.

4. In contrast, humidification–dehumidification technologies yielded the poorest ϕ_{2nd} values because it involves the AWH conversion process, so this technology is not recommended for further development.

5. Overall, AWH technologies have a much higher E_{Min} and lower ϕ_{2nd} values than desalination. The ideal ϕ_{2nd} needed by an AWH technology to make its energy performance comparable to desalination is at least 89.9%, which is almost impossible to practically achieve. Thus, from an energy standpoint, desalination is always preferred when a water reserve is available.

CRediT authorship contribution statement

Trevor Hocksun Kwan: Developed the black box minimum SEC model, Reported the minimum SEC curves, Conducted the energy optimality analysis of the various freshwater separation technologies, Wrote the initial manuscript. **Shuang Yuan:** Collected the SEC data as needed for the comparative analysis, Assisted in revising the manuscript contents. **Yongting Shen:** Collected the SEC data as needed for the comparative analysis, Assisted in revising the manuscript contents. **Gang Pei:** Funding, Supervised the team in carrying out this work.

Declaration of competing interest

The authors declare that they have no known competing financial interests or personal relationships that could have appeared to influence the work reported in this paper.

Data availability

No data was used for the research described in the article.

Acknowledgments

This research was sponsored by the Natural Science Foundation of Hefei, China (Grant No. 2021048) and the Fundamental Research Funds for the Central Universities, China (No. WK2090 000021).

Appendix

A.1. Humid air RH to water molar fraction conversion

When freshwater is being extracted from the humid air that consists of water and air as the constituents (i.e. $n = [n_{H_2O}, n_{air}]$), the term relative humidity is very often used to define the quantity of contained water, which should be converted into the molar fraction of water as required by the SEC model. First, the partial pressure of water can be calculated as follows:

$$p_{H_2O} = RH \times p_{H_2O(s)}(T) \tag{6}$$

where $p_{H_2O(s)}(T)$ is the saturation pressure of water at temperature T, which may be viewed as the pressure required to boil water at that temperature. After p_{H_2O} is known, the molar fraction of water can be calculated as follows:

$$\overline{n_{H_2O}} = \frac{p_{H_2O}}{P_0} \tag{7}$$

Meanwhile, the $h_{(i,k)}$ and $s_{(i,k)}$ values are found from accessing the thermophysical property library of the CoolProp package for 'water' and 'air', respectively. Hence, with the above two equations and a given recovery rate value, the variation of E_{Min} with RH, T and P_0 can be calculated.

Table A.1
The specific enthalpy and entropy of the two selected salts under standard ambient conditions.

Salt Type	Specific Enthalpy	Specific Entropy
NaCl (Ahmadi et al., 2016)	−411.2 kJ/mol	72.1 kJ/mol
$CaCl_2$ (Damo et al., 2019)	−795.4 kJ/mol	108.4 J/(mol K)

A.2. Salinity to water molar fraction conversion

When extracting from salt solutions, the involved constituents would be water and salt (i.e., $n = [n_{H_2O}, n_{Salt}]$). Conventionally, the seawater salt concentration by mass (C_{salt}) is used as the indicator for concentration level, which can be converted into water molar fraction by the following formula:

$$\overline{n_{H_2O}} = \frac{(1 - C_{Salt})\, M_{Salt}}{M_{H_2O} + (1 - C_{Salt})(M_{Salt} - M_{H_2O})} \tag{8}$$

where M_{Salt} and M_{H_2O} are the molar fractions of the water and salt materials, respectively. Similar to the AWH scenario, the $h_{(i,k)}$ and $s_{(i,k)}$ values of water are taken from the CoolProp package, but data for salts are not available there. Instead, the standard thermodynamic properties of the salts from available tables are used, as summarized in Table A.1. Specifically, the salts NaCl and $CaCl_2$ are selected because NaCl is the main component of the salt existing in seawater, while $CaCl_2$ is commonly used for water absorption purposes, as seen in some of the desiccant-based AWH technologies.

A.3. Calculating input heat based on the GOR

In many studies about desalination technologies, the Gain Output Ratio (GOR) is often used to quantify its energy performance. Here, formulations are provided to show how the SEC can be estimated with a given GOR value. Initially, the energy consumption of the technology can be calculated as follows:

$$Q_{In} = \frac{\dot{m}_w h_{fg}(T)}{GOR} \tag{9}$$

where $\dot{m}_w$ is the freshwater flow rate (kg/s in this formula), and h_{fg} is the latent heat of specific enthalpy at the boiling temperature T.

A.4. Calculating the "specific exergy consumption" from SEC

Usually, most publications will present the SEC results as 1st law values with the energy type possibly being heat, power, solar energy, etc. Indeed, different energy forms with differing conditions will involve different percentages of work. Therefore, a conversion into equivalent exergy is required to ensure a fair comparison, so this research defines a "specific exergy consumption" term (denoted as equivalent E) that universally expresses the total work content available at the input. To achieve this,

Table A.2
Comparison of the reported SEC and E_{min} values of various previous works relating to the AWH technology. If the recovery rate value is not available, then it is assumed to be 50%.

Type	ID	Reference	Operating Conditions	Reported Values	Equivalent E
Thermoelectric Cooler (TEC)	1	(Shourideh et al., 2018)	T = 30°C, RH = 60%	2002 Wh/kg (elec.)	2002 Wh/kg
	2	(Pontious et al., 2016)	T = 29.4°C, RH = 69.6%	1560 Wh/kg (elec.)	1560 Wh/kg
	3	(Eslami et al., 2018)	T = 45°C, RH = 75%	769 Wh/kg (elec.)	769 Wh/kg
	4	(Vián et al., 2002)	T = 27°C, RH = 80%	2243 Wh/kg (elec.)	2243 Wh/kg
	5	(Jradi et al., 2012)	T = 29.5°C, RH = 80%	2150 Wh/kg (PV elec.)	2150 Wh/kg
	6	(Liu et al., 2017)	T = 23.6°C, RH = 92.7%	2319 Wh/kg (elec.)	2319 Wh/kg
Vapor Compression Cycle (VCC)	7	(Zolfagharkhani et al., 2018a)	T = 30°C, RH = 50%	300 Wh/kg (elec.)	300 Wh/kg
	8	(Patel et al., 2020)	T = 35°C , RH = 95%	750 Wh/kg (elec.)	750 Wh/kg
	9	(Luo et al., 2004)	T = 26.7°C, RH = 50%	690 Wh/kg (elec.)	690 Wh/kg
	10	(Bagheri, 2018b)	T = 20°C, RH = 75%	1173 Wh/kg (elec.)	840 Wh/kg
Solar thermal liquid desiccant (ST-LD)	11	(Kabeel, 2007)	T = 29°C, RH = 60%	1496.6 Wh/kg (solar)	1724.1 Wh/kg
	12	(Wang et al., 2019a)	T = 30°C, RH = 80%	1851.85 Wh/kg (solar)	1330.4 Wh/kg
	13	(Elashmawy, 2020)	T = 32°C, RH = 68.86%; 0.467 L/(m^2 day) at reported 603 W/m^2 average irradiance over 12 h.	15495 Wh/kg (solar)	14426 Wh/kg
Solar thermal solid desiccant (ST-SD)	14	(Li et al., 2020a)	T = 25°C, RH = 80%	1333 Wh/kg (solar)	1241 Wh/kg
	15	(Li et al., 2018)	T = 26°C, RH = 65%	1408 Wh/kg	1311 Wh/kg
	16	(Kim et al., 2018)	T = 25°C, RH = 20%	3134 Wh/kg	2915 Wh/kg
	17	(Wang et al., 2018)	T = 25°C, RH = 75%	2300 Wh/kg	2139 Wh/kg
Hybrid Technologies (HT)	18	(Fill et al., 2020)	T = 25°C, RH = 31.5%; Reverse Osmosis -Desiccant	1173 Wh/kg (elec.)	1173 Wh/kg
	19	(Tu and Hwang, 2019)	T = 40°C, RH = 10%; VCC – Desiccant Wheel	793.65 Wh/kg (elec.)	793.65 Wh/kg
	20	(Al Keyyam et al., 2021)	T = 40°C, RH = 100% CPV/T – Stirling Engine – Absorption Cooling	225 Wh/L (elec.)	225 Wh/kg

the specific energy consumption results shall be multiplied with the appropriate formula that converts the energy magnitudes into their equivalent exergies. For example, the specific exergy consumption based on an input heat source is calculated as follows:

$$E = E_{(Heat)} \times (1 - \frac{T_0}{T_H}) \tag{10}$$

where T_0 (K) is the ambient temperature (the same term as that used in the W_{Min} calculation at Eqs. (2)), and T_H is the input heat's temperature (K). For example, if T_0 = 298.15 K (25 °C) and T_H = 383.15 K (110 °C), then the ratio is calculated to be $E = E_{Heat} \times \left(1 - \frac{298.15}{383.15}\right) = 0.2218E_{Heat}$.

For solar energy, the following equation can be used (taken from Gong and Wall (2014)):

$$E = E_{(Solar)} \times [1 + \frac{1}{3}\left(\frac{T_0}{T_{Sun}}\right)^4 - \frac{4}{3}\left(\frac{T_0}{T_{Sun}}\right)] \tag{11}$$

where T_{Sun} is the surface temperature of the Sun, which can be taken to be 5800 K. As a result, if T_0 = 298.15 K (25 °C), it can be found that $E_{2nd} = 0.931E_{(solar)}$.

Finally, because electricity and mechanical energy are equivalent to exergy, their reported SEC values directly equal the corresponding specific exergy consumption (i.e. $E = E_{(elec)} = E_{(mech)}$).

A.5. Table of reference data

This section shows the tables that detail the references that were used in Fig. 9 (for AWH in Table A.1) and Fig. 11 (for desalination in Table A.3) of the energy optimality analysis. In both tables, the reported energy consumption values are first provided and then converted into equivalent specific exergy consumptions (Equivalent E column) via the conversion equations from Section A3.

Table A.3
Comparison of the reported SEC and E_{min} values of previously studied desalination technologies. If the recovery rate value is not available, then it is assumed to be 50%, whereas if the study did not report the C_{salt} condition, then C_{salt} is assumed to be 3.5%, which corresponds to the average natural oceanic condition.

Type	ID	Ref.	Operating Conditions	Reported Values	Equivalent E
Multi-effect Distillation (MED)	1	(Abid et al., 2021b)	C_{salt} = 3.5%, T = 22.5 °C, RR = 33.96%, 4 effect	173.32 Wh/kg Heat at 120 °C	42.98 Wh/kg
	2	(Elsayed et al., 2018a)	C_{salt} = 4.2% T = 31.5 °C, 4 effect	136.7 Wh/ kg (Heat at 80 °C)	18.77 Wh/kg
	3	(Khalilzadeh and Hossein Nezhad, 2018)	C_{salt} = 4.2%, T = 25 °C, 6 effect	124.40 Wh/kg (Heat at 140 °C)	34.63 Wh/kg
	4	(Elsayed et al., 2018b)	C_{salt} = 3.5%, T = 31.5 °C	176.33 Wh/kg (Heat at 65 °C)	17.47 Wh/kg
	5	(Ghenai et al., 2021)	C_{salt} = 4.2%T = 25 °C, 1 effect	144.4743 Wh/kg (Heat at 80 °C)	22.5 Wh/kg
	6	(Ghenai et al., 2021)	C_{salt} = 4.2%, T = 25 °C, 9 effect	60.9838 Wh/kg (Heat at 80 °C)	9.498 Wh/kg
Multi-flash stage (MSF) Desalination	7	(Hanshik et al., 2016)	C_{salt} = 3.5% T = 25 °C, 3 effect	204 Wh/kg (Heat at 110 °C)	42.256 Wh/kg
	8	(Al-Othman et al., 2018)	C_{salt} = 4.8% T = 25 °C, 4 effect	33.51Wh/kg (Equiv. Exergy)	33.51Wh/kg
	9	(Rosso et al., 1996)	C_{salt} = 5.7%, T = 35 °C, 16 effect	96.62 Wh/kg (Heat at 110 °C)	18.913 Wh/kg
Multi-effect Membrane Distillation (MEMD)	10	(Boutikos et al., 2017)	C_{salt} = 3.5% RR = 40% T = 25 °C	252.5 Wh/kg (Heat at 90 °C)	45.2 Wh/kg
	11	(Ma et al., 2020)	C_{salt} = 3.84% T = 30 °C	68.5 Wh/kg (Heat at 80 °C)	9.698 Wh/kg
	12	(Andrés-mañas et al., 2020)	C_{salt} = 3.5% T = 25 °C	250 Wh/kg (Solar)	232.75 Wh/kg
Reverse Osmosis (RO)	13	(El Mansouri et al., 2020)	C_{salt} = 3.77%, T = 20 °C, RR = 40%	2.1 Wh/kg (Elec.)	2.1 Wh/kg
	14	(Lai et al., 2021)	C_{salt} = 3.5% T = 25 °C, RR = 65.5%	3.10 Wh/kg (Elec.)	3.10 Wh/kg
	15	(Peñate et al., 2011)	C_{salt} = 3.817% T = 20 °C, RR = 40%	2.78 Wh/kg (Elec.)	2.78 Wh/kg
	16	(Bilton et al., 2011)	C_{salt} = 3.5% T = 25 °C	3.25 Wh/kg (Elec.)	3.25 Wh/kg
	17	(Cerci, 2002)	C_{salt} = 0.155%, T = 15 °C, RR = 77.53%	0.52698 Wh/kg (Elec.)	0.52698 Wh/kg
Humidification-Dehumidification (HD)	18	(Ashrafizadeh and Amidpour, 2012)	C_{salt} = 3.5%, T = 30 °C	115.56 Wh/kg (Equiv. Exergy)	115.56 Wh/kg
	19	(Lawal et al., 2018b)	C_{salt} = 3.5% T = 27 °C	210 Wh/kg (Equiv. Exergy)	210 Wh/kg
	20	(Thanaiah et al., 2021)	C_{salt} = 3.5%, T = 30 °C	1028.16 Wh/kg (Heat at 100 °C)	192.87 Wh/kg

References

Abid, A., Jamil, M.A., Sabah, N.U., Farooq, M.U., Yaqoob, H., Khan, L.A., Shahzad, M.W., 2021a. Exergoeconomic optimization of a forward feed multi-effect desalination system with and without energy recovery. Desalination 499.

Abid, A., Jamil, M.A., Sabah, N.U., Farooq, M.U., Yaqoob, H., Khan, L.A., Shahzad, M.W., 2021b. Exergoeconomic optimization of a forward feed multi-effect desalination system with and without energy recovery. Desalination 499, 114808.

Ahmadi, M.H., Mohammadi, A., Pourfayaz, F., Mehrpooya, M., Bidi, M., Valero, A., Uson, S., 2016. Thermodynamic analysis and optimization of a waste heat recovery system for proton exchange membrane fuel cell using transcritical carbon dioxide cycle and cold energy of liquefied natural gas. J. Nat. Gas Sci. Eng. 34, 428–438.

Al-Fulaij, H.F., 2011. Dynamic Modeling of Multi Stage Flash (MSF) Desalination Plant Doctor of. University College London.

Al-Karaghouli, A., Kazmerski, L.L., 2013. Energy consumption and water production cost of conventional and renewable-energy-powered desalination processes. Renew. Sustain. Energy Rev. 24, 343–356.

Al Keyyam, I., Al-Nimr, M.D., Khashan, S., Keewan, A., 2021. A new solar atmospheric water harvesting integrated system using CPV/T – Stirling engine – Absorption cooling cycle and vapor compression refrigeration cycle. Int. J. Energy Res. 45, 16400–16417.

Al-Othman, A., Tawalbeh, M., El Haj Assad, M., Alkayyali, T., Eisa, A., 2018. Novel multi-stage flash (MSF) desalination plant driven by parabolic trough collectors and a solar pond: A simulation study in UAE. Desalination 443, 237–244.

Alharbi, S., Elsayed, M.L., Chow, L.C., 2020. Exergoeconomic analysis and optimization of an integrated system of supercritical CO2 Brayton cycle and multi-effect desalination. Energy 197.

Altaee, A., Mabrouk, A., Bourouni, K., Palenzuela, P., 2014. Forward osmosis pretreatment of seawater to thermal desalination: High temperature FO-MSF/MED hybrid system. Desalination 339, 18–25.

Anbarasu, T., Pavithra, S., 2011. Vapour compression refrigeration system generating fresh water from humidity in the air.

Andrés-mañas, J.A., Roca, L., Ruiz-Aguirre, A., Acién, F.G., Gil, J.D., Zaragoza, G., 2020. Application of solar energy to seawater desalination in a pilot system based on vacuum multi-effect membrane distillation. Appl. Energy 258.
Ashrafizadeh, S.A., Amidpour, M., 2012. Exergy analysis of humidification–dehumidification desalination systems using driving forces concept. Desalination 285, 108–116.
Atta RM, E.A., 2011. Solar water condensation using thermoelectric coolers. Int. J. Water Resour. Arid. Environ. 1, 142–145.
Bagheri, F., 2018a. Performance investigation of atmospheric water harvesting systems. Water Resour. Ind. 20, 23–28.
Bagheri, F., 2018b. Performance investigation of atmospheric water harvesting systems. Water Resour. Ind. 20, 23–28.
Belessiotis V., E.D., 1999. The history of renewable energies for water desalination. Desalination 128, 147–159.
Beyrami, J., Chitsaz, A., Parham, K., Arild, Ø., 2019. Optimum performance of a single effect desalination unit integrated with a SOFC system by multi-objective thermo-economic optimization based on genetic algorithm. Energy 186, 115811-115811.
Bilton, A.M., Kelley, L.C., Steven, D., 2011. Photovoltaic reverse osmosis - Feasibility and a pathway to develop technology. Desalin. Water Treat. 31, 24–34.
Boutikos, P., Mohamed, E.S., Mathioulakis, E., Belessiotis, V., 2017. A theoretical approach of a vacuum multi-effect membrane distillation system. Desalination 422, 25–41.
Burn, S., Hoang, M., Zarzo, D., Olewniak, F., Campos, E., Bolto, B., Barron, O., 2015. Desalination techniques — A review of the opportunities for desalination in agriculture. Desalination 364, 2–16.
Cerci, Y., 2002. Exergy analysis of a reverse osmosis desalination plant in California. Desalination 142, 257–266.
Chen, Z., Shi, J., Li, Y., Ma, B., Yan, X., Liu, M., Jin, H., Li, D., Jing, D., Guo, L., 2021. Recent progress of energy harvesting and conversion coupled with atmospheric water gathering. Energy Convers. Manage. 246.
Clus, O., Ortega, P., Muselli, M., Milimouk, I., Beysens, D., 2008. Study of dew water collection in humid tropical islands. J. Hydrol. 361, 159–171.
Cunha, D.P.S., Pontes, K.V., 2022. Desalination plant integrated with solar thermal energy: A case study for the Brazilian semi-arid. J. Clean. Prod. 331.
Damo, U.M., Ferrari, M.L., Turan, A., Massardo, A.F., 2019. Solid oxide fuel cell hybrid system: A detailed review of an environmentally clean and efficient source of energy. Energy 168, 235–246.
Ejeian, M., Wang, R.Z., 2021. Adsorption-based atmospheric water harvesting. Joule 5, 1678–1703.
El Mansouri, A., Hasnaoui, M., Amahmid, A., Hasnaoui, S., 2020. Feasibility analysis of reverse osmosis desalination driven by a solar pond in Mediterranean and semi-arid climates. Energy Convers. Manage. 221, 113190.
El-Zanati, E., El-Khatib, K.M., 2007. Integrated membrane –based desalination system. Desalination 205, 15–25.
Elashmawy, M., 2020. Experimental study on water extraction from atmospheric air using tubular solar still. J. Clean. Prod. 249, 119322-119322.
Elashmawy, M., Alshammari, F., 2020a. Atmospheric water harvesting from low humid regions using tubular solar still powered by a parabolic concentrator system. J. Clean. Prod. 256, 120329-120329.
Elashmawy, M., Alshammari, F., 2020b. Atmospheric water harvesting from low humid regions using tubular solar still powered by a parabolic concentrator system. J. Clean. Prod. 256.
Elsayed, M.L., Mesalhy, O., Mohammed, R.H., Chow, L.C., 2018a. Exergy and thermo-economic analysis for MED-TVC desalination systems. Desalination 447, 29–42.
Elsayed, M.L., Mesalhy, O., Mohammed, R.H., Chow, L.C., 2018b. Transient performance of MED processes with different feed configurations. Desalination 438, 37–53.
Eslami, M., Tajeddini, F., Etaati, N., 2018. Thermal analysis and optimization of a system for water harvesting from humid air using thermoelectric coolers. Energy Convers. Manage. 174, 417–429.
Fill, M., Muff, F., Kleingries, M., 2020. Evaluation of a new air water generator based on absorption and reverse osmosis. Heliyon 6, e05060-e05060.
Geng, D., Cui, J., Fan, L., 2021. Performance investigation of a reverse osmosis desalination system powered by solar dish-Stirling engine. Energy Rep. 7, 3844–3856.
Ghaffour, N., Missimer, T.M., Amy, G.L., 2013. Technical review and evaluation of the economics of water desalination: Current and future challenges for better water supply sustainability. Desalination 309, 197–207.
Ghenai, C., Kabakebji, D., Douba, I., Yassin, A., 2021. Performance analysis and optimization of hybrid multi-effect distillation adsorption desalination system powered with solar thermal energy for high salinity sea water. Energy 215.
Gido, B., Friedler, E., Broday, D.M., 2016. Liquid-desiccant vapor separation reduces the energy requirements of atmospheric moisture harvesting. Environ. Sci. Technol. 50, 8362–8367.
Gong, M., Wall, G., 2014. Life cycle exergy analysis of solar energy systems. J. Fundam. Renew. Energy Appl. 5.
Hanshik, C., Jeong, H., Jeong, K.-W., Choi, S.-H., 2016. Improved productivity of the MSF (multi-stage flashing) desalination plant by increasing the TBT (top brine temperature). Energy 107, 683–692.
Hassan, A., Al-Dadah, R., Mahmoud, S., Fath, H., Hussien, E., Genidi, N., 2020. Integration of vacuum multi effect membrane distillation with adsorption/cooling system. Appl. Therm. Eng. 178.
He, W.F., Xu, L.N., Han, D., Gao, L., Yue, C., Pu, W.H., 2016. Thermodynamic investigation of waste heat driven desalination unit based on humidification dehumidification (HDH) processes. Appl. Therm. Eng. 100, 315–324.
Hua, L., Xu, J., Wang, R., 2021. Nano Energy Exergy-efficient boundary and design guidelines for atmospheric water harvesters with nano-porous sorbents. Nano Energy 85, 105977-105977.
Jamil, M.A., Zubair, S.M., 2018. Effect of feed flow arrangement and number of evaporators on the performance of multi-effect mechanical vapor compression desalination systems. Desalination 429, 76–87.
Jradi, M., Ghaddar, N., Ghali, K., 2012. Experimental and theoretical study of an integrated thermoelectric–photovoltaic system for air dehumidification and fresh water production. Int. J. Energy Res. 36, 963–974.
Kabeel, A.E., 2007. Water production from air using multi-shelves solar glass pyramid system. Renew. Energy 32, 157–172.
Kavitha, J., Rajalakshmi, M., Phani, A.R., Padaki, M., 2019. Pretreatment processes for seawater reverse osmosis desalination systems—A review. J. Water Process. Eng. 32.
Khalil, B., Adamowski, J., Shabbir, A., Jang, C., Rojas, M., Reilly, K., Ozga-Zielinski, B., 2016. A review: dew water collection from radiative passive collectors to recent developments of active collectors. Sustain. Water Resour. Manag. 2, 71–86.
Khalilzadeh, S., Hossein Nezhad, A., 2018. Utilization of waste heat of a high-capacity wind turbine in multi effect distillation desalination: Energy, exergy and thermoeconomic analysis. Desalination 439, 119–137.
Kim, H., Rao, S.R., Kapustin, E.A., Zhao, L., Yang, S., Yaghi, O.M., Wang, E.N., 2018. Adsorption-based atmospheric water harvesting device for arid climates. Nature Commun. 9 (1191).
Kim, H., Yang, S., Rao, S.R., Narayanan, S., Kapustin, E.A., Furukawa, H., Umans, A.S., Yaghi, O.M., Wang, E.N., 2017. Water harvesting from air with metal–organic frameworks powered by natural sunlight. Science 356, 430–434.
Kwan, T.H., Shen, Y., Hu, T., Gang, P., 2020. Passively improving liquid sorbent based atmospheric water generation by integration of fuel cell waste products. J. Clean. Prod..
Lai, X., Long, R., Liu, Z., Liu, W., 2021. Solar energy powered high-recovery reverse osmosis for synchronous seawater desalination and energy storage. Energy Convers. Manage. 228.
Lapotin, A., Zhong, Y., Zhang, L., Zhao, L., Leroy, A., Kim, H., Rao, S.R., Wang, E.N., 2020. Dual-stage atmospheric water harvesting device for scalable solar-driven water production. Joule.
Lawal, D.U., Zubair, S.M., Antar, M.A., 2018a. Exergo-economic analysis of humidification-dehumidification (HDH) desalination systems driven by heat pump (HP). Desalination 443, 11–25.
Lawal, D.U., Zubair, S.M., Antar, M.A., 2018b. Exergo-economic analysis of humidification-dehumidification (HDH) desalination systems driven by heat pump (HP). Desalination 443, 11–25.
Lee, H.S., 2010. Thermal Design: Heat Sinks, Thermoelectrics, Heat Pipes, Compact Heat Exchangers, and Solar Cells. Wiley.
Li, W., Dong, M., Fan, L., John, J.J., Chen, Z., Fan, S., 2020b. Nighttime radiative cooling for water harvesting from solar panels. ACS Photonics.
Li, R. A.-O., Shi, Y., Alsaedi, M., Wu, M., Shi, L., Wang, P. A.-O., 2018. Hybrid Hydrogel with High Water Vapor Harvesting Capacity for Deployable Solar-Driven Atmospheric Water Generator.
Li, R., Shi, Y., Wu, M., Hong, S., Wang, P., 2019. Improving atmospheric water production yield: Enabling multiple water harvesting cycles with nano sorbent. Nano Energy 10425, 5–104255.
Li, R., Shi, Y., Wu, M., Hong, S., Wang, P., 2020a. Improving atmospheric water production yield: Enabling multiple water harvesting cycles with nano sorbent. Nano Energy 67, 104255.
Lin, S., Zhao, H., Zhu, L., He, T., Chen, S., Gao, C., Zhang, L., 2021. Seawater desalination technology and engineering in China: A review. Desalination 498.
Liu, Shanshan, H., W., Hu, Dengyun, Lv, Song, Chen, Delu, Wu, Xin, Xu, Fusuo, Li, Sijia, 2017. Experimental analysis of a portable atmospheric water generator by thermoelectric cooling method. Energy Procedia 142, 1609–1614.
Liu, J.Y., W.J., Wang, L.W., Qi, Y., 2016. Performance test of sorption air-to-water device. CIE J. 67, 46–50.
Luo, J.J., Z.W., Bai, Xb, 2004. Development and application of a field water maker. Heat Vent Air Cond 34, 42–45.
Ma, M., Liang, W., Wang, S., Xie, Q., Qian, D., Bai, Z., Zhang, T., Zhang, R., 2020. A pure-conduction transient model for heat pipes via derivation of a pseudo wick thermal conductivity. Int. J. Heat Mass Transfer 149.

Maestre-Valero, J.F., Martínez-alvarez, V., Baille, A., Martín-górriz, B., Gallego-Elvira, B., 2011. Comparative analysis of two polyethylene foil materials for dew harvesting in a semi-arid climate. J. Hydrol. 410, 84–91.
Mahjoob Karambasti, B., Ghodrat, M., Ghorbani, G., Lalbakhsh, A., Behnia, M., 2022. Design methodology and multi-objective optimization of small-scale power-water production based on integration of Stirling engine and multi-effect evaporation desalination system. Desalination 526, 115542-115542.
Mendoza-Escamilla, A.J., Hernandez-Rangel, J.F., Cruz-alcántar, P., Saavedra-Leos, Z.M., Morales-Morales, J., Figueroa-Diaz, A.R., Valencia-Castillo, M.C., Martinez-Lopez, J.F., 2019. A feasibility study on the use of an atmospheric water generator (AWG) for the harvesting of fresh water in a semi-arid region affected by mining pollution. Appl. Sci. 9.
Moharram, N.A., Bayoumi, S., Hanafy, A.A., El-Maghlany, W.M., 2021a. Hybrid desalination and power generation plant utilizing multi-stage flash and reverse osmosis driven by parabolic trough collectors. Case Stud. Therm. Eng. 23.
Moharram, N.A., Bayoumi, S., Hanafy, A.A., El-Maghlany, W.M., 2021b. Techno-economic analysis of a combined concentrated solar power and water desalination plant. Energy Convers. Manage. 228.
Pangarkar, B.L., Deshmukh, S.K., 2015. Theoretical and experimental analysis of multi-effect air gap membrane distillation process (ME-AGMD). J. Environ. Chem. Eng. 3, 2127–2135.
Patel, J., Patel, K., Mudgal, A., Panchal, H., Sadasivuni, K.K., 2020. Experimental investigations of atmospheric water extraction device under different climatic conditions. Sustain. Energy Technol. Assess. 38, 100677-100677.
Peñate, B., Castellano, F., Bello, A., García-Rodríguez, L., 2011. Assessment of a stand-alone gradual capacity reverse osmosis desalination plant to adapt to wind power availability: A case study. Energy 36, 4372–4384.
Pontious, K., Weidner, B., Guerin, N., Dates, A., Pierrakos, O., Altaii, K., 2016. Design of an atmospheric water generator: Harvesting water out of thin air. In: 2016 IEEE Systems and Information Engineering Design Symposium (SIEDS).
Qi, H., Wei, T., Zhao, W., Zhu, B., Liu, G., Wang, P., Lin, Z., Wang, X., Li, X., Zhang, X., Zhu, J., 2019. An interfacial solar-driven atmospheric water generator based on a liquid sorbent with simultaneous adsorption–desorption. Adv. Mater. 31, 1903378.
Rosso, M., A.B., Mazzotti, M., 1996. Modeling multistage flash desalination plants. Desalination 108, 365–374.
Rostamzadeh, H., Nourani, P., 2019. Investigating potential benefits of a salinity gradient solar pond for ejector refrigeration cycle coupled with a thermoelectric generator. Energy 172, 675–690.
Salehi, A.A., Ghannadi-Maragheh, M., Torab-Mostaedi, M., Torkaman, R., Asadollahzadeh, M., 2020. A review on the water-energy nexus for drinking water production from humid air. Renew. Sustain. Energy Rev. 120.
Salek, F., Eshghi, H., Zamen, M., Ahmadi, M.H., 2022. Energy and exergy analysis of an atmospheric water generator integrated with the compound parabolic collector with storage tank in various climates. Energy Rep. 8, 2401–2412.
Santosh, R., Lee, H.-S., Kim, Y.-D., 2022. A comprehensive review on humidifiers and dehumidifiers in solar and low-grade waste heat powered humidification-dehumidification desalination systems. J. Clean. Prod. 347.
Seader, J.D., Henley, E.J., Roper, D.K., 1998. Separation Process Principles. wiley, New York.
Shahzad, M.W., M.B., Ang, L., Ng, K.C., 2018. Sustainable Desalination. Elsevier Inc.
Shalaby, S.M., Sharshir, S.W., Kabeel, A.E., Kandeal, A.W., Abosheiasha, H.F., Abdelgaied, M., Hamed, M.H., Yang, N., 2022. Reverse osmosis desalination systems powered by solar energy: Preheating techniques and brine disposal challenges – A detailed review. Energy Convers. Manage. 251, 114971.
Sharaf Eldean, M.A., Fath, H.E., 2013. Exergy and thermo-economic analysis of solar thermal cycles powered multi-stage flash desalination process. Desalin. Water Treat. 51, 7361–7378.
Shourideh, A.H., Bou Ajram, W., Al Lami, J., Haggag, S., Mansouri, A., 2018. A comprehensive study of an atmospheric water generator using Peltier effect. Therm. Sci. Eng. Progr. 6, 14–26.
Siegel, N.P., Conser, B., 2021. A techno-economic analysis of solar-driven atmospheric water harvesting. J. Energy Resour. Technol. 143.
Smejkal, T., Mikyška, J., Fučík, R., 2020. Numerical modelling of adsorption and desorption of water vapor in zeolite 13X using a two-temperature model and mixed-hybrid finite element method numerical solver. Int. J. Heat Mass Transfer 148, 119050-119050.
Srivastava, S., Yadav, A., 2018. Water generation from atmospheric air by using composite desiccant material through fixed focus concentrating solar thermal power. Sol. Energy 169, 302–315.
Talaat, M.A., Awad, M.M., Zeidan, E.B., Hamed, A.M., 2018. Solar-powered portable apparatus for extracting water from air using desiccant solution. Renew. Energy 119, 662–674.
Tayyeban, E., Deymi-Dashtebayaz, M., Dadpour, D., 2022. Multi objective optimization of MSF and MSF-TVC desalination systems with using the surplus low-pressure steam (an energy, exergy and economic analysis). Comput. Chem. Eng. 160, 107708-107708.
Terlouw, T., Alskaif, T., Bauer, C., Van Sark, W., 2019. Optimal energy management in all-electric residential energy systems with heat and electricity storage. Appl. Energy 254, 113580-113580.
Thanaiah, K., Gumtapure, V., Mitiku Tadesse, G., 2021. Experimental analysis on humidification-dehumidification desalination system using different packing materials with baffle plates. Therm. Sci. Eng. Progr. 22.
Tu, R., Hwang, Y., 2019. Performance analyses of a new system for water harvesting from moist air that combines multi-stage desiccant wheels and vapor compression cycles. Energy Convers. Manage. 198, 111811-111811.
Tu, R., Hwang, Y., 2020. Reviews of atmospheric water harvesting technologies. Energy 201, 117630-117630.
Uddin, M.K., Shammi, M., Islam, M.S., Saadat, A.H.M., Sultana, A., Islam, M.S., 2018. Desalination technologies for developing countries: A review. J. Sci. Res. 10, 77–97.
Vián, J.G., Astrain, D., Domınguez, M., 2002. Numerical modelling and a design of a thermoelectric dehumidifier. Appl. Therm. Eng. 22, 407–422.
Wang, X., Li, X., Liu, G., Li, J., Hu, X., Xu, N., Zhao, W., Zhu, B., Zhu, J., 2019a. An interfacial solar heating assisted liquid sorbent atmospheric water generator. Angew. Chem. Int. Ed. Engl. 58, 12054–12058.
Wang, X., Li, X., Liu, G., Li, J., Hu, X., Xu, N., Zhao, W., Zhu, B., Zhu, J., 2019b. An interfacial solar heating assisted liquid sorbent atmospheric water generator. Angew. Chem. Int. Edn 58, 12054–12058.
Wang, L., Violet, C., Duchanois, R.M., Elimelech, M., 2020. Derivation of the theoretical minimum energy of separation of desalination processes. J. Chem. Educ.
Wang, J.Y., Wang, R.Z., Tu, Y.D., Wang, L.W., 2018. Universal scalable sorption-based atmosphere water harvesting. Energy 165, 387–395.
Woo, Y.C., Kim, S.-H., Shon, H.K., Tijing, L.D., 2019. Introduction: Membrane desalination today, past, and future. Curr. Trends Future Dev. (Bio-) Membr.
Yu, J., Wang, Y., 2022. Policies on seawater desalination and water security in China: Evolution, challenges and recommendations for the future. J. Clean. Prod. 336.
Zhang, T., W.R., Yan, T., Wang, L., Lin, C.H., 2010. Development of portable Air-based water collector for field operations under conditions of severe water shortage. Chin. Med. Equip. J. 31, 70–72.
Zhao, R., Deng, S., Liu, Y., Zhao, Q., He, J., Zhao, L., 2017. Carbon pump: Fundamental theory and applications. Energy 119, 1131–1143.
Zhao, K., Heinzl, W., Wenzel, M., Büttner, S., Bollen, F., Lange, G., Heinzl, S., Sarda, N., 2013. Experimental study of the memsys vacuum-multi-effect-membrane-distillation (V-MEMD) module. Desalination 323, 150–160.
Zhou, L., Li, X., Ni, G.W., Zhu, S., Zhu, J., 2019. The revival of thermal utilization from the Sun: Interfacial solar vapor generation. Natl. Sci. Rev. 6, 562–578.
Zhou, X., Lu, H., Zhao, F., Yu, G., 2020. Atmospheric water harvesting: A review of material and structural designs. ACS Mater. Lett. 2, 671–684.
Zolfagharkhani, S., Zamen, M., Shahmardan, M.M., 2018a. Thermodynamic analysis and evaluation of a gas compression refrigeration cycle for fresh water production from atmospheric air. Energy Convers. Manage. 170, 97–107.
Zolfagharkhani, S., Zamen, M., Shahmardan, M.M., 2018b. Thermodynamic analysis and evaluation of a gas compression refrigeration cycle for fresh water production from atmospheric air. Energy Convers. Manage. 170, 97–107.

Further reading

Chernikov, A.A., 2011. Artificial rainfall. Hydrol. Cycle 11.